Supplementary Material for
Noise Modeling in One Hour: Minimizing Preparation Efforts for Self-supervised Low-Light RAW Image Denoising

A. Quantum efficiency of modern imaging sensors

Here, we present the typical fill-factor-included spectral-averaging quantum efficiency (QE) of modern imaging sensors. Specifically, we plot the QE values of 393 different camera models sourced from DxOMark[1] and summarized by Photons to Photos[2]. As illustrated in Fig. A, a dominant portion of sensors exhibits QE values in the range of $(30\%, 70\%)$. Another noteworthy observation is that sensor models with QE values lower than 30% were typically released before (or around) the year 2010. This timestamp marks a transition from front-illuminated CMOS sensors to back-illuminated counterparts, leading to a substantial increase in QE. To conclude, the analysis of QE reinforces our hypothesis-based shot noise synthesis method as being generally applicable, particularly for modern sensors.

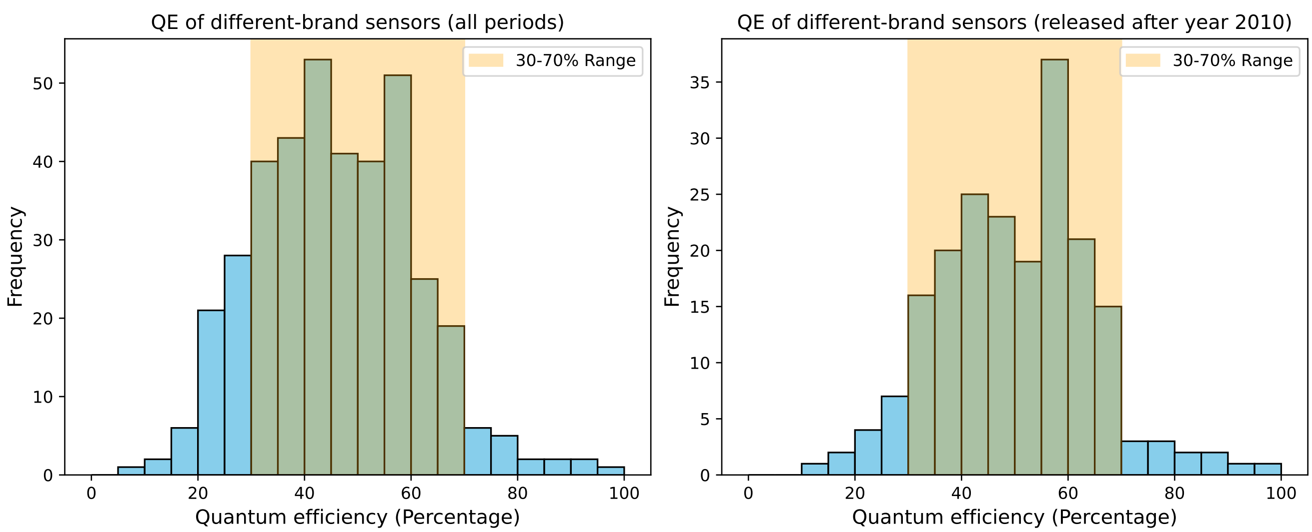

Figure A. Quantum efficiency statistics of different-brand imaging sensors. There are 393 data points in total, with 204 representing models released later than the year 2010. Although some data points appear to be outliers (*e.g.*, there unlikely exists a CMOS sensor with a 100% QE), we keep them in the plots to stick to the original data.

B. Importance of different noise components

Here, we study the importance of different components in noise synthesis for training the denoising network. We use the SID and ELD datasets for experimental setup and disable different noise components during noise synthesis. As summarized in Table A, neither shot nor signal-independent noise can be omitted from the noise synthesis pipeline, otherwise, the denoising performance would diminish significantly. Also, dark shading plays an important role in improving the denoising accuracy.

[1] https://www.dxomark.com/

[2] https://www.photonstophotos.net/Charts/Sensor_Characteristics.htm

Table A. Denoising performance w.r.t. different noise components used during synthesis.

Noise component used in synthesis			**SID**		**ELD**	
Photon shot noise	Sampled dark frame	Dark shading correction	PSNR	SSIM	PSNR	SSIM
✓			39.81	0.9182	44.95	0.9613
	✓		39.95	0.9412	44.90	0.9708
✓	✓		40.14	0.9438	45.49	0.9786
	✓	✓	40.37	0.9436	45.60	0.9788
✓		✓	38.12	0.8922	44.16	0.9673
✓	✓	✓	40.85	0.9478	46.43	0.9834

C. More denoising results

We present more qualitative denoising results achieved with our noise synthesis pipeline. As illustrated in Fig. B, our proposal can help the denoising network effectively smooth real-world noisy images in various scenarios without losing many high-frequency details.

References

[1] C. Chen, Q. Chen, J. Xu, and V. Koltun, "Learning to see in the dark," in *CVPR*, 2018. 3

[2] K. Wei, Y. Fu, Y. Zheng, and J. Yang, "Physics-based noise modeling for extreme low-light photography," *IEEE TPAMI*, vol. 44, no. 11, pp. 8520–8537, 2021. 3

[3] H. Feng, L. Wang, Y. Wang, H. Fan, and H. Huang, "Learnability enhancement for low-light raw image denoising: A data perspective," *IEEE TPAMI*, vol. 46, no. 1, pp. 370–387, 2024. 3

Figure B. Qualitative denoising results achieved by our proposed method on distinct datasets. All images are brightness-adjusted via a digital gain, and gamma-corrected for better visualization.